ACS APPLIED MATERIALS & INTERFACES

www.acsami.org

Forum Article

Transduction of Amine−Phosphate Supramolecular Interactions and Biosensing of Acetylcholine through PEDOT-Polyamine Organic Electrochemical Transistors

Marjorie Montero-Jimenez,[⊥] Juan Lugli-Arroyo,[⊥] Gonzalo E. Fenoy, Esteban Piccinini,* Wolfgang Knoll, Waldemar A. Marmisollé,* and Omar Azzaroni

Cite This: https://doi.org/10.1021/acsami.3c09286

Read Online

ACCESS | Metrics & More | Article Recommendations | Supporting Information

ABSTRACT: Organic electrochemical transistors (OECTs) are important devices for the development of flexible and wearable sensors due to their flexibility, low power consumption, sensitivity, selectivity, ease of fabrication, and compatibility with other flexible materials. These features enable the creation of comfortable, versatile, and efficient portable devices that can monitor and detect a wide range of parameters for various applications. Herein, we present OECTs based on PEDOT-polyamine thin films for the selective monitoring of phosphate-containing compounds. Our findings reveal that supramolecular single phosphate−amino interaction induces higher changes in the OECT response compared to ATP−amino interactions, even at submillimolar concentrations. The steric character of binding anions plays a crucial role in OECT sensing, resulting in a smaller shift in maximum transconductance voltage and threshold voltage for bulkier binding species. The OECT response reflects not only the polymer/solution interface but also events within the conducting polymer film, where ion transport and concentration are affected by the ion size. Additionally, the investigation of enzyme immobilization reveals the influence of phosphate species on the assembly behavior of acetylcholinesterase (AchE) on PEDOT-PAH OECTs, with increasing phosphate concentrations leading to reduced enzyme anchoring. These findings contribute to the understanding of the mechanisms of OECT sensing and highlight the importance of careful design and optimization of the biosensor interface construction for diverse sensing applications.

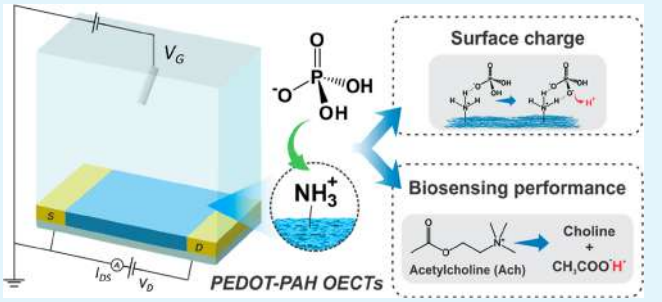

KEYWORDS: *Organic electrochemical transistors, PEDOT, Conducting polymers, Biosensors, Acetylcholine, Amino−phosphate interactions*

INTRODUCTION

Supramolecular (i.e., noncovalent) interactions play an essential role in a wide variety of functions, ranging from the formation of colloids, metabolic processes, and medical therapies to biosensing applications such as wearable and flexible monitoring.[1−5] The *in situ* monitoring of the components participating in supramolecular interactions is of great importance to better understand and, thus, design, develop, or optimize the applications that involve them.[6,7] In particular, the association between polyamines and phosphates is an important type of supramolecular bond that has significant implications in various biological systems.[8−10] Although electrostatic interactions are the primary driving force for the creation of polyamine−phosphate assemblies,[11] hydrogen bonds are also believed to play a crucial role in stabilizing their structure.[12,13] One example is the formation of nuclear aggregates of biogenic polyamines, such as putrescine, spermidine, and spermine, and orthophosphate anions (Pi) in many replicating cells.[10] These aggregates hierarchically assemble into cyclic structures with high order that can protect DNA.[14] Additionally, diatom biosilica is mainly composed of polyamines that have up to 20 repeated units and silaffins. Their interaction with phosphate anions (which act as ionic cross-linkers) produces aggregates that determine the species-specific patterning of diatom biosilica.[15] Polyamine−phosphate-based systems have also been employed for constructing drug delivery platforms.[16] Similarly, poly(allylamine)-Pi (PAH-Pi) nanoparticles have been used as carriers for silencing RNAs.[17] Furthermore, polyamine−phosphate interactions have been used to create supramolecular films which can modulate cell adhesion and

Special Issue: Flexible Bioelectronics with a Focus on Europe

Received: June 27, 2023
Accepted: September 27, 2023

proliferation,[18] or integrate redox enzymes for biosensing applications.[19]

On the other hand, organic electrochemical transistors (OECTs) have emerged as a promising class of devices for bioelectronic applications due to their unique properties such as high interfacial sensitivity and offering scalable manufacturing of flexible and miniaturized sensing arrays.[20−22] These devices consist of an organic semiconductor film that spans source and drain electrodes and whose conductivity can be regulated by the application of a gate voltage (V_G) through an electrolyte.[23,24] This device configuration allows recording signals using a V_G of maximum transconductance, a condition of major importance for sensors with improved sensitivity.[25] Moreover, the transconductance can be augmented by molecular doping, increase of degree of crystallinity, and film thickness, among other approaches. On the other hand, the need for ion injection from the electrolyte to maintain charge balance limits the response time.[26] The conducting channel material most commonly used in OECTs is poly(3,4-ethylenedioxythiophene) (PEDOT) as well as its water-stable colloidal complex with poly(styrenesulfonate) (PEDOT:PSS).[27] However, PEDOT's intrinsic doping yields depletion mode operation, necessitating high operating currents and gate voltages to keep the channel in the OFF state, which can trigger parasitic reactions and lead to device deterioration.[28] Another problem to overcome concerns the integration of the semiconductor with biological entities toward the development of bioelectronic devices. In this sense, the absence of functional groups in pristine PEDOT films hampers the integration of OECTs with biological entities.[29,30] Additionally, the excess of PSS in PEDOT:PSS films results in a negatively charged surface that limits their interfacing with most proteins, nucleic acids, and cells.[31]

Therefore, in the last years, researchers have explored different methods to tailor the surface of PEDOT and PEDOT:PSS films.[32] A particularly interesting approach involves the incorporation of amines moieties to the channel material, thus conferring anchoring sites for further biofunctionalization of the conducting polymer.[33,34] In this context, the recent development of OECTs employing PEDOT:TOS and poly(allylamine hydrochloride) (PAH) composites as conducting channel materials represents a significant advancement in the field.[35,36] The regulation of the PAH:PEDOT ratio allows for the straightforward tuning of both electronic and ionic transport of the devices, producing transistors with low threshold voltages while maintaining high transconductance values. Moreover, the pH-sensitive amino moieties in the PEDOT matrix improve the pH response of the transistors and enable the nondenaturing electrostatic anchoring of functional enzymes such as acetylcholinesterase (AchE).[34]

In this regard, recent studies have indicated that interactions between phosphate and amino groups can impede the adsorption of enzymes such as glucose oxidase and urease on polyamine-modified surfaces.[12,37] As the concentration of phosphate in the enzyme buffer solution increases, the amount of immobilized protein decreases significantly due to the interaction between the polyamine-modified surface and the phosphate species in the electrolyte. Hence, the study of the interactions of polyamines with phosphate anions in OECTs is of major relevance, showing important consequences for the biosensing field.

Finally, concerning previous works on this matter, the effect of Pi−amino interactions on the transfer characteristics of polyamine-modified graphene field effect transistors and their influence on the performance of urea biosensors have been recently described.[37] Regarding organic transistors, and very recently, Mitobe et al. reported the fabrication of an extended gate OFET-based platform for the detection of various phosphate species such as pyrophosphate, adenosine monophosphate, and adenosine triphosphate.[38] However, to the best of our knowledge, the incidence of polyamine−phosphate interactions on the OECTs has not been studied so far.

In this work, OECTs are designed and manufactured to allow for the in situ monitoring of compounds with phosphate groups and, through the incorporation of enzymes, the biologically catalyzed biosensing of acetylcholine. The transistors were prepared based on PEDOT-PAH thin films as channel transistors using a one-pot strategy by chemical oxidation of EDOT in the presence of poly(allylamine) (PAH). The incorporation of PAH and its functional impact are evidenced by Raman characterization and field effect measurements at different pH values, respectively. To evaluate the sensing characteristics and transduction capacity, field effect measurements were performed, both transfer characteristics and transient experiments. By a systematic field effect study in the presence of different phosphate salts and other divalent anions, the selective affinity against phosphate groups, the influence of the size of the anion, and the utility of the transistor as a device to transduce molecular recognition were demonstrated. In contrast to other previously studied devices, such as graphene-based field-effect transistors[37] or solid-state nanochannels,[39] where the effects of surface charge reversion induced by specific phosphate ion binding dominate the changes in response, in the case of OECTs, interpreting the results requires considering not only surface aspects but also ion transport through the polymer film. Lastly, the electrostatic integration of the acetylcholinesterase enzyme for the biosensing of acetylcholine was performed, and the impact of the presence of phosphate salts during the enzyme immobilization protocol on the biosensor performance was evaluated.

MATERIALS AND METHODS

Reagents and Materials. Poly(allylamine hydrochloride) (PAH) (17.5 kDa, lot no. MKBW4380 V, St. Louis, MO, USA), 3,4-ethylenedioxythiophene (EDOT) (lot no. WXBC1309 V, Wuxi, China), acetylcholine chloride (≥99%), sodium tripolyphosphate (TPP) (85%), and acetylcholinesterase (AchE) from *Electrophorus electricus* (≥1000 units/mg protein) were obtained from Sigma-Aldrich. Fe (III) p-toluenesulfonate (Fe (III) Tos) (38−42% in n-butanol) was purchased from Heraeus. Pyridine, butanol, and potassium dihydrogen phosphate (KH_2PO_4) were obtained from Biopack. Potassium chloride (KCl) and HEPES were purchased from Anedra, and adenosine-5′-triphosphate disodium salt (ATP) was purchased from Calzyme. Interdigitated Au electrodes (IDEs) with a 10/10 μm electrode/gap (ED-IDE1-Aul) deposited on glass substrates were purchased from Micrux (Spain). The distance that separates the IDEs (channel length) is 10 μm, and the total contour of the IDEs (channel width) is 23.5 cm.

Fabrication of OECTs and Films. PEDOT and PEDOT-PAH films were prepared by *in situ* oxidative chemical polymerization onto glass and IDEs employing a Spin Coater WS-650MZ-23NPP instrument (Laurell Tech. Corp.).[34] For the fabrication of the OECTs, IDEs were first cleaned with acetone and ethanol. Then, for PEDOT OECTs, an oxidant solution containing 715 μL of Fe (III) Tos, 220 μL of butanol, and 16.5 μL of pyridine was used to

https://doi.org/10.1021/acsami.3c09286
ACS Appl. Mater. Interfaces XXXX, XXX, XXX−XXX

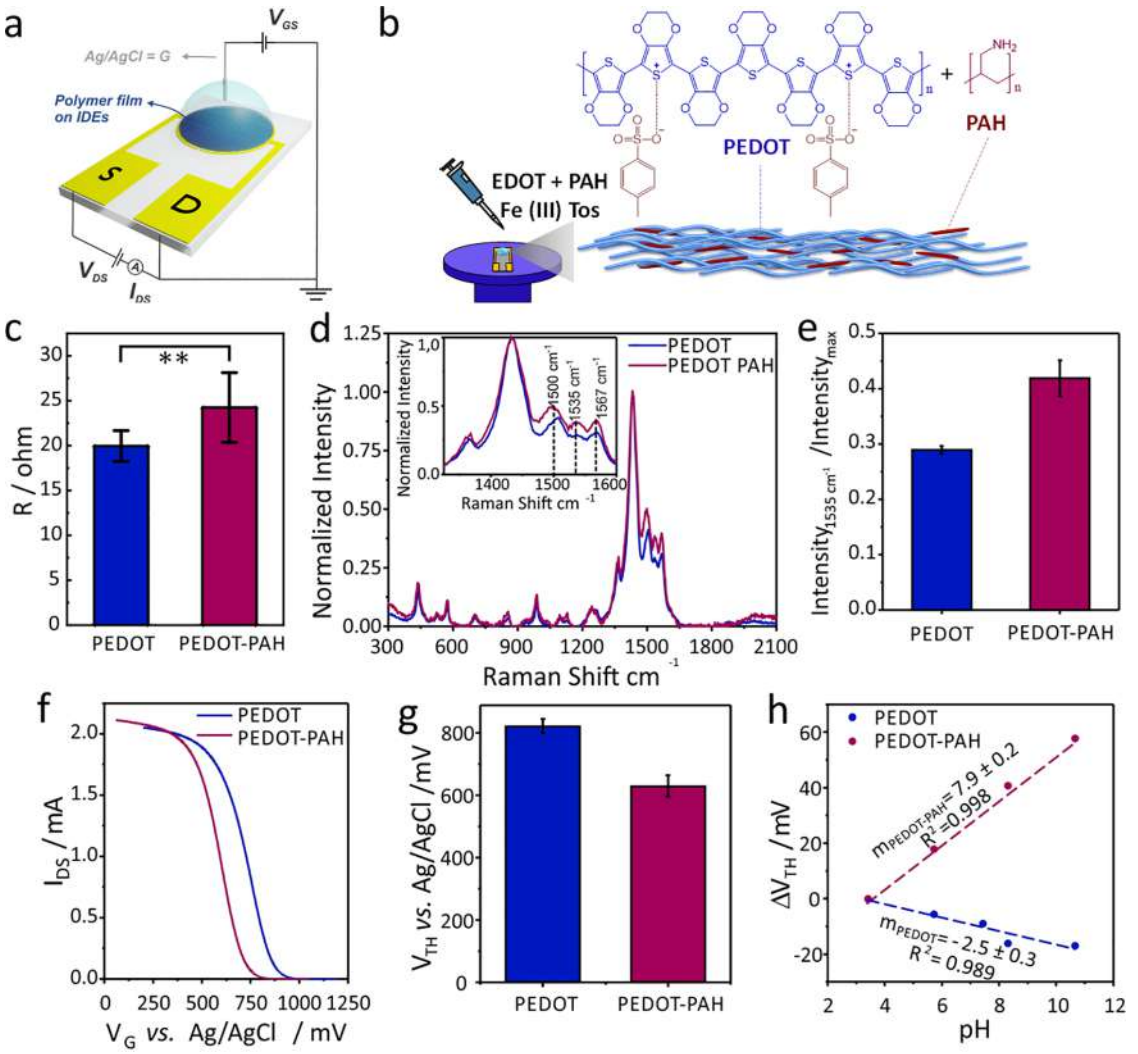

Figure 1. (a) Scheme of the OECTs configuration. (b) Scheme of the production of PEDOT and PEDOT-PAH films by spin coating. (c) Resistance measurements of PEDOT and PEDOT-PAH OECTs (N = 10 for both systems). Level of significance is shown as $^{**}p < 0.05$. (d) Raman spectra measured on PEDOT (blue) and PEDOT-PAH (purple) films. (e) Ratio of Raman intensity at 1535 cm^{-1} regarding the maximum intensity peak (1430 cm^{-1}). (f) Characteristic transfer curves of PEDOT and PEDOT-PAH transistors (0.1 M KCl, pH 7.4). (g) Threshold potential determined for PEDOT and PEDOT-PAH OECTs (N = 10). (h) Threshold potential shift as a function of pH for PEDOT and PEDOT-PAH OECTs. Data were obtained from three independent measurements. Dashed lines are the linear fits of the data. (b, d, and f) Error bars correspond to the standard deviation.

polymerize 12.5 μL of EDOT. The solution was homogenized and filtered (pore size 0.2 μm). For PEDOT-PAH OECTs, 200 μL of PAH solution was added in this step (15 mg of PAH in 200 μL of Milli-Q water). Straight away, the solution was spin coated onto the array area of the IDEs, at 1000 rpm for 1 min (acceleration 500 rpm min^{-1}). No mask was employed, so all of the area of the IDE was covered by the polymerization solution. Next, in order to promote the polymerization, electrodes were heated at 70 °C on a hot plate for 20 min. The metal contact points were cleaned by using a swab soaked in ethanol. Finally, they were washed with distilled water and dried in compressed air. The channel thickness of the PEDOT-PAH transistors has been previously determined via AFM measurements by scratching with a sharp razor blade in a perpendicular orientation with respect to the IDEs.[34] The obtained channel thickness was 114 ± 2 nm.

Raman Spectroscopy. Raman spectra were acquired from PEDOT and PEDOT-PAH films synthesized on glass substrates. The measurements were carried out with an i-Raman BW415−532S (BWTek) Raman spectrometer at 532 nm as laser wavelength and with a power of 40 mW and 4 cm^{-1} resolution. The samples were in the focus of a 20× optical microscope (BAC151B, BWTek) and then measured at three different spots. The spectral region was analyzed from 75 to 4000 cm^{-1}. The BWSpec 4 Software was employed for background removal with the same procedure for all the samples.

Electrochemical Measurement. The transfer curves (drain-source current vs gate potential) were obtained with a TEQ bipotensiostat. The measurements were made in a top-gated architecture (Figure 1a). The drain-source current (I_{DS}) was measured, while the gate potential (V_G) was scanned at 10 mV s^{-1} from 50 to 1050 mV, and the drain-source potential (V_{DS}) was set at −50 mV. The electrolyte solution was 0.1 M KCl, and the gate used was an Ag/AgCl wire. In order to obtain the threshold voltage (V_{TH}) for each OECT, the transfer characteristic curves were plotted and fitted to a linear regime from 75% $I_{DS,max}$ to 25% $I_{DS,max}$. Later, $V_{DS}/2$ was added to the obtained extrapolated value at I_{DS}= 0, as previously reported.[34]

Fabrication and Evaluation of OECTs Biosensors. AchE stock solution was prepared using 0.5 mg of enzyme in 1 mL of buffer solution (10 mM KCl and 0.1 mM HEPES, pH 7.4). The electrostatic anchoring was performed using a previous reported protocol.[34,35] Briefly, the PEDOT-PAH OECTs were immersed into the enzyme

https://doi.org/10.1021/acsami.3c09286
ACS Appl. Mater. Interfaces XXXX, XXX, XXX−XXX

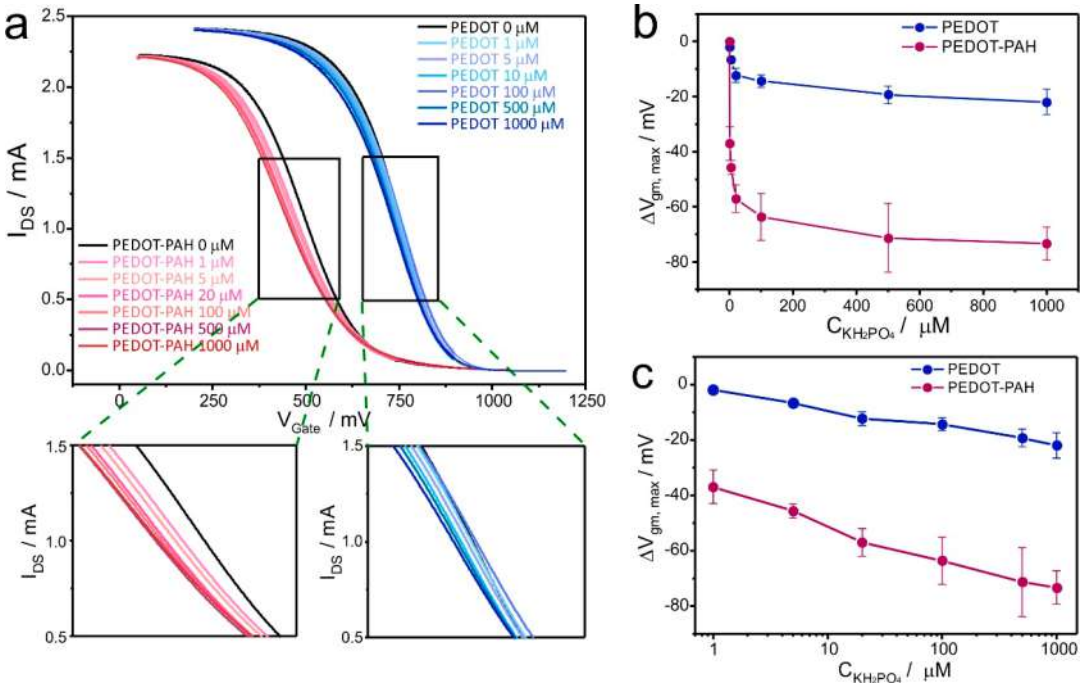

Figure 2. (a) Transfer curves of PEDOT and PEDOT-PAH transistors at increasing concentration of KH_2PO_4, 0.1 M KCl, and pH 7 and (b, c) its respective change of maximum transconductance potential with phosphate concentration. Concentration scale in plot c allows a better reading at low Pi concentrations. Bars correspond to the SD of 3 different OECTs.

solution for 30 min. Then they were rinsed with a buffer solution and stored at 4 °C.

With the aim of assessing the effect of Pi−amino interactions on the enzyme anchoring (and therefore on the performance of the biosensors), the electrostatic anchoring of the enzyme to the PEDOT-PAH OECTs was also performed by adding 1 mM KH_2PO_4 to the buffer solution while performing the same steps. Next, the performance of the biosensors was evaluated by the measurement of transfer curves in solutions with increasing concentrations of acetylcholine chloride. Three transfer curves were recorded for each Ach concentration.

RESULTS AND DISCUSSION

PEDOT and PEDOT-PAH OECTs were prepared by *in situ* oxidative chemical polymerization via a spin coating procedure (Figure 1b). The air resistance of the deposited film on the IDEs between both D and S electrodes was measured in order to corroborate the proper formation of the polymer films (Figure 1c, sample size measured n = 10). PAH brings functional groups that ease the functionalization of the OECTs such as the anchoring of biological elements.[34] However, PAH itself is a non-conductive electrochemically inactive block; then the integration of PAH to PEDOT matrix produced an increment of electrical resistance from 20 to 24 Ω.[34,40]

Additionally, Raman spectroscopy measurements were performed to characterize the chemical nature of the films. In Figure 1d, the normalized Raman spectra of PEDOT and PEDOT-PAH films are shown. The obtained spectra show typical bands of PEDOT films with different degrees of doping. The main peaks are observed in the region 1300−1600 cm^{-1} with a sharpest band at 1430 cm^{-1}, corresponding to the C_α=C_β(−O) symmetric stretching.[41] Spectra in Figure 1d were normalized regarding the maximum intensity of this peak to simplify the comparison. As observed, the dominant changes caused by the integration of PAH appear in the 1500−1600 cm^{-1} range. These results are consistent with previous works.[35,42] The asymmetric bands of the C_α=C_β(−O) stretching have been reported to appear split into two contributions at about 1500 and 1567 cm^{-1}, respectively, and shifted to higher energies upon electrochemical doping.[41] The peak observed at 1506 cm^{-1} for PEDOT films moved to 1498 cm^{-1} when the PAH was added to the polymer, indicating that the PEDOT doping level reduces. Also, the relative increase of the band at 1535 cm^{-1} becomes indicative of a lower doping degree of the polymer.[43] Figure 1e shows the relative intensity at 1535 cm^{-1} of PEDOT and PEDOT-PAH films (each sample was measured at three different spots). Then the integration of the polyamine to the PEDOT matrix yields a decrease in the degree of doping of PEDOT.

The transfer characteristic curves of the OECTs were recorded by measuring the drain-source current (I_{DS}) while scanning the gate voltage (V_G). Figure 1f shows the transfer curves for the PEDOT and PEDOT-PAH-based transistors. As observed, the addition of PAH leads to a shift of the transfer curves to lower gate voltages. Additionally, the output characteristics curves corroborate that in the working range of V_G, the transistor goes from the "on" (potential to the maximum current occurs) to the "off" (potential to which no current flows) mode (Figure S1). The threshold potential (V_{TH}), which is the minimum potential required to start the reaction involved in the OECT system, in this case the oxidation of semiconductor polymer, shifted from 822 to 629 mV (Figure 1g).

The shift caused by the integration of PAH has been previously observed in PEDOT-based OECTs, and it has been assigned to both the increase in the ionic conductivity and the dedoping promoted by the interaction with amine groups.[34] In this regard, an enhancement of the ionic conductivity within the films has been observed by integrating polyelectrolytes to PEDOT-based composites.[44] It has even been reported that the incorporation of polycations to PEDOT/PSS composites

https://doi.org/10.1021/acsami.3c09286
ACS Appl. Mater. Interfaces XXXX, XXX, XXX−XXX

also improves the electronic conductivity by promoting structural changes in the PEDOT domains.[45] On the other hand, the incorporation of aliphatic amines to the PEDOT conducting channel has been reported to cause a reduction in the doping degree leading to a shifting of the characteristic curves to lower V_G values.[46,47] This last idea is consistent with Raman results, indicating a lower doping degree by the polyamine integration. Thus, with PAH being a polycation with primary amine groups, the addition of PAH to the PEDOT conducting composites would improve the ionic conductivity but would also reduce the doping degree of PEDOT. The product between the charge mobility (μ) and the capacitance per unit of volume (C^*) was obtained as previously reported (see calculation details in the Supporting Information, SI).[26] A μC^* product of 0.51 F cm^{-1} V^{-1} s^{-1} was obtained for the PEDOT-PAH OECTs. This value is higher than PEDOT:PMATFSILi80[48] and p(gNDI-g2T)[49] but lower than PEDOT:DS + EG.[50]

Additionally, the inherent nature of PAH being a weak polyelectrolyte further contributes to the pH responsiveness of the composite. In this regard, the pH dependence of PEDOT and PEDOT-PAH transistors response was evaluated using solutions with increasing values of pH. It is observed that as pH increases, the curves for PEDOT-OECTs slightly shift to lower V_G values, whereas the curves for PEDOT-PAH films shift to higher V_G values, with a more pronounced pH dependence (transfer curves are shown in Figure S3). In Figure 1h, these differences are characterized in terms of the shifting of the threshold potentials (ΔV_{TH}, see the SI for calculation details) for both types of OECTs. Slopes of the linear fittings reported in this figure reflect the enhanced pH sensitivity of the PEDOT-PAH OECTs, indicating that amino groups in the conducting channel are available for the protonation/deprotonation process according to the pH of the solution.[33]

EFFECT OF PHOSPHATE SPECIES ON THE OECT PERFORMANCE

Figure 2a shows the transfer curves for PEDOT and PEDOT-PAH transistors recorded in 0.1 M KCl with different concentrations of inorganic phosphate (Pi) at pH 7. At this pH, the main species present in the electrolyte are $H_2PO_4^-$/HPO_4^{2-}. A shift of the transfer curves to lower values of V_G as the phosphate concentration increases can be observed for both PEDOT and PEDOT-PAH-based OECTs. However, it is clearly observed that PEDOT-PAH OECTs present a higher sensitivity to the Pi concentration (insets in Figure 2a).

The transconductance (g_m) is the sensitivity of the I_{DS} shift with respect to changes of V_G ($g_m = dI_{DS}/dV_G$). Then, in order to quantify the shift on transfer curves, the maximum transconductance potential ($V_{gm,max}$) was determined as the maximum value from the dI_{DS}/dV_G curve, that corresponds to $dg_m/dV_G = 0$. At $V_{gm,max}$ the drain-source current shifts are more sensitive to changes in the gate potential. The obtained values as a function of the phosphate concentration are shown on a linear and logarithmic scale in Figures 2b and c. Average results from the measurements of three independent X-ray emissions of OECTs are reported.

The decrease of the $\Delta V_{gm,max}$ values with the increase of Pi concentration observed for PEDOT-PAH can be attributed to the interaction between the amine and phosphate groups, respectively. Therefore, at pH 7, monovalent and divalent species of phosphate are in equilibrium, but the $H_2PO_4^-$/HPO_4^{2-} proportion of surface bound phosphate species can be affected by the interaction with amino groups of the PAH. In this regard, it has been proposed that the interaction between amino groups and Pi species favors the Pi deprotonation, which would lead to a higher ionic charge contribution from phosphate anions.[39]

The effect of Pi−amino interactions on the transfer characteristics of polyamine-modified graphene-based field effect transistors has been recently described, showing the specificity of the interaction and the effect on the transfer curves of the devices.[37]

In order to evaluate the specificity of the Pi−amino interactions on the OECT performance, transfer curves were also recorded by adding other divalent anions (in the sub milimolar concentration range) to 0.1 M KCl electrolyte. Next, sulfate (SO_4^{2-}) and oxalate ($C_2O_4^{-2}$) ions were used as divalent anions.[12,39] Considering that the pK_a values of both anions are 1.99 and 4.27, respectively, it is assumed that they are completely dissociated at pH 7. Figure 3a shows that

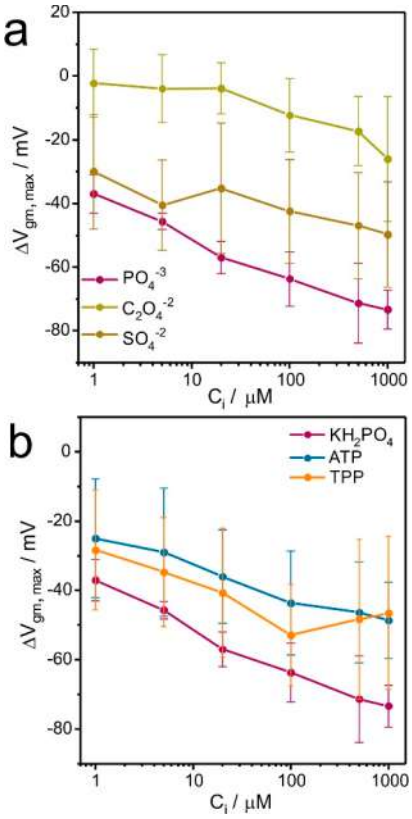

Figure 3. Variation of maximum transconductance potential of PEDOT-PAH OECTs in the presence of increasing concentration of (a) different anions: phosphate, sulfate, and oxalate; and (b) different phosphate species: KH_2PO_4, ATP, and TPP (0.1 M KCl, pH 7). Bars correspond to the SD of 3 different OECTs.

phosphate anions present greater shifts in maximum transconductance potential compared with the other divalent anions used (see the SI for statistical analysis). This finding indicates that the nature of the amino−phosphate interaction is not completely electrostatic, but specific interactions (such as hydrogen bonds) with the composite components would also be important. In this regard, the importance of hydrogen bonds between amine and phosphate groups has been assigned as responsible for the specific interaction observed.[12,51−53] Although SO_4^{2-} and $C_2O_4^{-2}$ are completely dissociated,

https://doi.org/10.1021/acsami.3c09286
ACS Appl. Mater. Interfaces XXXX, XXX, XXX−XXX

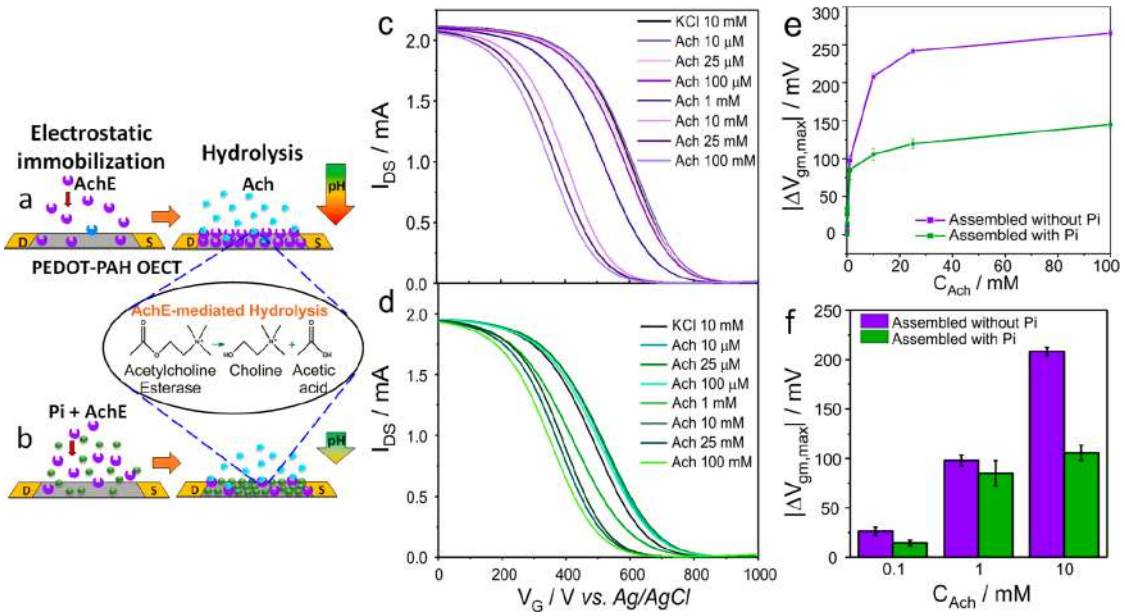

Figure 4. Assembly of biosensor in the (a) absence and (b) presence of Pi. Transfer curves of AchE/PEDOT-PAH OECT recorded in solutions of increasing acetylcholine chloride concentrations (10 mM KCl, 0.1 mM HEPES pH 7.4), the enzyme deposition was carried out in the (c) absence and (d) presence of 1m KH_2PO_4. (e) Changes of maximum transconductance potential ($V_{gm,max\ Ci} - V_{gm,max\ Co}$) as a function of the acetylcholine concentration (error bars correspond to measurements made with the same OECT $N = 3$) . (f) Comparison of the variation of maximum transconductance potential at selected substrate concentrations.

sulfates present greater $\Delta V_{gm,max}$, which could be associated with the steric character since oxalate is bigger than sulfate, hindering the interaction with amino groups.[54,55]

The specific interaction with amino species was further studied by analyzing the influence of more complex phosphate anions on the response of PEDOT-PAH OECTs. Figure 3b shows the influence of adenosine triphosphate (ATP) and tripolyphosphate anion (TPP). Both ATP and TPP are molecules of biomedical interest. ATP (adenosine triphosphate) is indeed responsible for various biological processes within cells. It serves as the primary energy source for cellular activities. The concentration of ATP can be associated with certain diseases such as hypoglycemia and malignant tumors. Meanwhile, tripolyphosphate anion (TPP) is frequently used as ionic cross-linker of chitosan to form complexes with potential applications as drugs delivery systems.[56,57]

Considering the dissociation of ATP at the working pH and the binding scheme sketched in eqs 1 and 2, a higher interaction of amine groups with both ATP and TPP compared with a single Pi species is expected:

$$\mathrm{ATP}^{-3}/\mathrm{ATP}^{-4} + (-\mathrm{NH_3})^{+} \rightarrow (-\mathrm{NH_3ATP})^{-2}/(-\mathrm{NH_3ATP})^{-3} \quad (1)$$

$$\mathrm{Pi}^{-1}/\mathrm{Pi}^{-2} + (-\mathrm{NH_3})^{+} \rightarrow (-\mathrm{NH_3Pi})^{0}/(-\mathrm{NH_3Pi})^{-1} \quad (2)$$

This trend has been systematically found when analyzing the influence of the phosphate species on the zeta-potential of PAH-modified microparticles,[12] the conductance of PAH-coated nanochannels,[39] and the functional response of PAH-coated gFETs.[37] However, in the present case, the Pi−amino interaction leads to higher changes in the OECT response than ATP−amino interactions, even in the submillimolar range. This point reinforces the hypothesis that the steric character of the binding of anions also plays an important role in the OECT sensing, leading to a smaller shift in $\Delta V_{gm,max}$ and ΔV_{TH} if the binding species are bulkier molecules. Effective radii values reported for Pi and ATP are ∼3 Å and ∼6 Å, respectively,[58] which indicate an effective volume 4-times higher for ATP compared with Pi. Moreover, the size of TPP molecule should be in between Pi and ATP, which is in line to the trend observed for the shift in $\Delta V_{gm,max}$ for TPP, being lower than the one observed for Pi but higher than that resulting for ATP. In addition, previous studies have shown that as the ion size increases there is an observed decrease of the concentration of ions within the polymer films.[55,59] Therefore, results in this work suggest that the OECT response reflects the physicochemical events occurring not only on the polymer/solution interface, which is the case for gFETs,[37] but also within the conducting polymer film. For OECTs, the ion size seems to play an important role in their transport and concentration inside the film and therefore in the transistor sensing performance. If the effect was solely due to the modification of the surface charge of the conducting channel (at the polymer/electrolyte interface) resulting from the binding of phosphate species, one would expect to observe a trend similar to that already reported for graphene-based transistors: ATP and TPP similarly bind to amino groups and produce a charge reversion more pronounced than that obtained with single Pi ions.[12,39] However, the differences in the response of the OECTs to the concentration of different phosphate species suggest that the effect operates not only at the polymer/solution interface.

IMPLICATIONS OF PHOSPHATE ASSOCIATION ON OECT BIOSENSORS CONSTRUCTION

We also studied the influence of inorganic phosphate species on the electrostatic assembly of an enzyme on the PEDOT-PAH transistors and the subsequent effect on the biosensor performance based on the OECT response. Previous works with urease found that the presence of Pi in the assembly

https://doi.org/10.1021/acsami.3c09286
ACS Appl. Mater. Interfaces XXXX, XXX, XXX−XXX

buffer reduces the amount of enzyme anchored to gFETs compared to the anchoring in Pi-free PBS.[37] In the present case, the enzyme acetylcholinesterase (AchE) was electrostatically immobilized on PEDOT-PAH OECTs by dip-coating, according to a recently reported protocol.[34] This procedure was carried out in the presence (Figure 4a) and absence (Figure 4b) of 1 mM KH_2PO_4 (0.1 mM HEPES, 10 mM KCl, pH 7.4). Then the biosensing performance of the enzyme functionalized OECTs was evaluated toward increasing concentrations of the enzyme substrate (acetylcholine). As shown in Figure 4c and d, it is possible to observe the detection of acetylcholine by the OECTs assembled in both conditions. In agreement with previous results, the transfer curves shift to more negative values due to the catalyzed acetylcholine hydrolysis, producing acetic acid and choline and, therefore, changing the local pH. These results indicate the presence of active enzyme bound to the PEDOT-PAH channel.[34]

A higher shift of the transfer curves can be observed if the biosensor is assembled in the absence of a phosphate species. Particularly, the variation in the maximum transconductance potential caused by the presence of the enzyme substrate is markedly higher for the assembly without phosphate, leading to appreciable changes in the biosensor response at different analyte concentrations (Figure 4e,f). This effect can be assigned to the screening of the adsorption of the negatively charged enzyme on the positively charged PEDOT-PAH surface by phosphate binding, even in the millimolar range. It has been previously shown that the presence of single phosphate anions hinders the electrostatic anchoring of the negatively charged enzyme glucose oxidase on PAH-functionalized surfaces[12] and also the assembly of negatively charged urease on PAH-coated gFETs[37] as a consequence of the charge reversion of the amine-functionalized surfaces by phosphate binding. The same phenomenon is also responsible for facilitating the assembly of positively charged cytochrome c on self-assembled monolayers (SAMs) of NH_2-terminated alcanethiols.[60]

It is important to note here that the phosphate concentration employed in this study is relatively low, corresponding to a 1/10 dilution of the commonly used PBS buffer. These findings further emphasize the caution required when using PBS or other phosphate-containing buffers for constructing interfacial architectures involving amino-bearing macromolecules through supramolecular interactions.

CONCLUSIONS

In summary, we have developed organic electrochemical transistors (OECTs) based on PEDOT-polyamine thin films that allow for the *in situ* and selective monitoring of compounds with phosphate groups. Transfer characteristics experiments were carried out in the presence of inorganic phosphate, as well as molecules of biomedical interest such as TTP and ATP. An observed decrease of the potential of maximum transconductance in the presence of these molecules can be attributed to the interaction between amine and phosphate groups. Interestingly, the devices exhibited a size-dependent response to phosphate molecules: Pi > TPP > ATP. This trend is different to that observed on nanochannels or gFETs, where the phosphate-amine binding affinity governs the response. Since OECT transduction occurs not only on the polymer film surface but also within the polymer thickness, it is suggested that the steric constraint of bulky ions and the decrease in ion mobility may be causing this behavior.

Furthermore, the enzyme acetylcholinesterase (AchE) was electrostatically immobilized on PEDOT-PAH OECTs for acetylcholine detection. We discovered that the immobilization of AchE on the PEDOT-PAH surface is significantly influenced by an increasing concentration of Pi in the enzyme solution, which can be attributed to Pi−amino interactions. Our findings demonstrate that even relatively low concentrations of Pi, such as those commonly found in 1/10 dilutions of PBS buffer, substantially reduce the amount of anchored AchE. The observed influence of phosphate species on the assembly behavior of enzymes further emphasizes the need for caution when employing PBS and other phosphate-containing solutions in the study of supramolecular systems involving amino-bearing entities.

ASSOCIATED CONTENT

Supporting Information

The Supporting Information is available free of charge at https://pubs.acs.org/doi/10.1021/acsami.3c09286.

Further electrochemical characterization of the PEDOT-PAH OECT and details of the calculations (PDF)

AUTHOR INFORMATION

Corresponding Authors

Esteban Piccinini − *Instituto de Investigaciones Fisicoquímicas Teóricas y Aplicadas (INIFTA), Departamento de Química, Facultad de Ciencias Exactas, Universidad Nacional de La Plata, La Plata B1904DPI, Argentina;* orcid.org/0000-0003-3270-7150; Email: estebanpiccinini@inifta.unlp.edu.ar

Waldemar A. Marmisollé − *Instituto de Investigaciones Fisicoquímicas Teóricas y Aplicadas (INIFTA), Departamento de Química, Facultad de Ciencias Exactas, Universidad Nacional de La Plata, La Plata B1904DPI, Argentina;* orcid.org/0000-0003-0031-5371; Email: wmarmi@inifta.unlp.edu.ar

Authors

Marjorie Montero-Jimenez − *Instituto de Investigaciones Fisicoquímicas Teóricas y Aplicadas (INIFTA), Departamento de Química, Facultad de Ciencias Exactas, Universidad Nacional de La Plata, La Plata B1904DPI, Argentina*

Juan Lugli-Arroyo − *Departamento de Química, Facultad de Ciencias Exactas, Universidad Nacional de La Plata, La Plata B1904DPI, Argentina*

Gonzalo E. Fenoy − *Instituto de Investigaciones Fisicoquímicas Teóricas y Aplicadas (INIFTA), Departamento de Química, Facultad de Ciencias Exactas, Universidad Nacional de La Plata, La Plata B1904DPI, Argentina;* orcid.org/0000-0003-4336-4843

Wolfgang Knoll − *Laboratory for Life Sciences and Technology (LiST), Faculty of Medicine and Dentistry, Danube Private University, 3500 Krems, Austria;* orcid.org/0000-0003-1543-4090

Omar Azzaroni − *Instituto de Investigaciones Fisicoquímicas Teóricas y Aplicadas (INIFTA), Departamento de Química, Facultad de Ciencias Exactas, Universidad Nacional de La Plata, La Plata B1904DPI, Argentina*

Complete contact information is available at:

https://doi.org/10.1021/acsami.3c09286
ACS Appl. Mater. Interfaces XXXX, XXX, XXX−XXX

https://pubs.acs.org/10.1021/acsami.3c09286

Author Contributions

⊥M.M-J. and J.L.A. contributed equally to this work.

Notes

The authors declare no competing financial interest.

■ ACKNOWLEDGMENTS

M.M.-J. acknowledges a scholarship from CONICET. E.P., W.A.M., and O.A. are staff members of CONICET and acknowledge the financial support from Universidad Nacional de La Plata (PPID-X867), CONICET (PIP-0370, PIP 11220210100209CO), and ANPCyT (PICT-2017- 1523, PICT2018-00780, PICT2018-4684, PICT-2020-02468, and PICT-2021-GRFTI-00042).

■ REFERENCES

(1) Steed, J. W.; Atwood, J. L. *Supramolecular Chemistry*, 2nd ed.; Steed, J. W., Atwood, J. L., Eds.; Wiley-VCH, 2009.
(2) Giménez, R. E.; Piccinini, E.; Azzaroni, O.; Rafti, M. Lectin-Recognizable MOF Glyconanoparticles: Supramolecular Glycosylation of ZIF-8 Nanocrystals by Sugar-Based Surfactants. *ACS Omega* **2019**, *4* (1), 842−848.
(3) Azzaroni, O.; Conda-Sheridan, M. *Supramolecular Nanotechnology: Advanced Design of Self-Assembled Functional Materials*; Azzaroni, O., Conda-Sheridan, M., Eds.; Wiley-VCH, 2023.
(4) Piccinini, E.; Allegretto, J. A.; Scotto, J.; Cantillo, A. L.; Fenoy, G. E.; Marmisollé, W. A.; Azzaroni, O. Surface Engineering of Graphene through Heterobifunctional Supramolecular-Covalent Scaffolds for Rapid COVID-19 Biomarker Detection. *ACS Appl. Mater. Interfaces* **2021**, *13* (36), 43696−43707.
(5) Yang, Y.; Gao, W. Wearable and Flexible Electronics for Continuous Molecular Monitoring. *Chem. Soc. Rev.* **2019**, *48* (6), 1465−1491.
(6) Kolesnichenko, I. V.; Anslyn, E. V. Practical Applications of Supramolecular Chemistry. *Chem. Soc. Rev.* **2017**, *46* (9), 2385−2390.
(7) Piccinini, E.; Bliem, C.; Giussi, J. M.; Knoll, W.; Azzaroni, O. Reversible Switching of the Dirac Point in Graphene Field-Effect Transistors Functionalized with Responsive Polymer Brushes. *Langmuir* **2019**, *35* (24), 8038−8044.
(8) Di Luccia, A.; Picariello, G.; Iacomino, G.; Formisano, A.; Paduano, L.; D'Agostino, L. The in Vitro Nuclear Aggregates of Polyamines. *FEBS J.* **2009**, *276* (8), 2324−2335.
(9) Marmisollé, W. A.; Irigoyen, J.; Gregurec, D.; Moya, S.; Azzaroni, O. Supramolecular Surface Chemistry: Substrate-Independent, Phosphate-Driven Growth of Polyamine-Based Multifunctional Thin Films. *Adv. Funct. Mater.* **2015**, *25* (26), 4144−4152.
(10) D'Agostino, L.; Di Luccia, A. Polyamines Interact with DNA as Molecular Aggregates. *Eur. J. Biochem.* **2002**, *269* (17), 4317−4325.
(11) Irigoyen, J.; Moya, S. E.; Iturri, J. J.; Llarena, I.; Azzaroni, O.; Donath, E. Specific ζ-Potential Response of Layer-by-Layer Coated Colloidal Particles Triggered by Polyelectrolyte Ion Interactions. *Langmuir* **2009**, *25* (6), 3374−3380.
(12) Laucirica, G.; Marmisollé, W. A.; Azzaroni, O. Dangerous Liaisons: Anion-Induced Protonation in Phosphate-Polyamine Interactions and Their Implications for Charge States of Biologically Relevant Surfaces. *Phys. Chem. Chem. Phys.* **2017**, *19*, 8612−8620.
(13) Herrera, S. E. S. E.; Agazzi, M. L. M. L.; Cortez, M. L. L.; Marmisollé, W. A. W. A.; Tagliazucchi, M.; Azzaroni, O. Polyamine Colloids Cross-Linked with Phosphate Ions: Towards Understanding the Solution Phase Behavior. *ChemPhysChem* **2019**, *20* (8), 1044−1053.
(14) Iacomino, G.; Picariello, G.; Sbrana, F.; Di Luccia, A.; Raiteri, R.; D'Agostino, L. DNA Is Wrapped by the Nuclear Aggregates of Polyamines: The Imaging Evidence. *Biomacromolecules* **2011**, *12* (4), 1178−1186.
(15) Kröger, N.; Deutzmann, R.; Bergsdorf, C.; Sumper, M. Species-Specific Polyamines from Diatoms Control Silica Morphology. *Proc. Natl. Acad. Sci. U. S. A.* **2000**, *97* (26), 14133−14138.
(16) Agazzi, M. L.; Herrera, S. E.; Cortez, M. L.; Marmisollé, W. A.; Azzaroni, O. Self-Assembled Peptide Dendrigraft Supraparticles with Potential Application in PH/Enzyme-Triggered Multistage Drug Release. *Colloids Surfaces B Biointerfaces* **2020**, *190*, No. 110895.
(17) Andreozzi, P.; Diamanti, E.; Py-Daniel, K. R.; Cáceres-Vélez, P. R.; Martinelli, C.; Politakos, N.; Escobar, A.; Muzi-Falconi, M.; Azevedo, R.; Moya, S. E. Exploring the PH Sensitivity of Poly(Allylamine) Phosphate Supramolecular Nanocarriers for Intracellular SiRNA Delivery. *ACS Appl. Mater. Interfaces* **2017**, *9* (44), 38242−38254.
(18) Muzzio, N. E.; Pasquale, M. A.; Marmisollé, W. A.; von Bilderling, C.; Cortez, M. L.; Pietrasanta, L. I.; Azzaroni, O. Self-Assembled Phosphate-Polyamine Networks as Biocompatible Supramolecular Platforms to Modulate Cell Adhesion. *Biomater. Sci.* **2018**, *6* (8), 2230−2247.
(19) Zappi, D.; Coria-Oriundo, L. L.; Piccinini, E.; Gramajo, M.; Von Bilderling, C.; Pietrasanta, L. I.; Azzaroni, O.; Battaglini, F. The Effect of Ionic Strength and Phosphate Ions on the Construction of Redox Polyelectrolyte-Enzyme Self-Assemblies. *Phys. Chem. Chem. Phys.* **2019**, *21* (41), 22947.
(20) Keene, S. T.; Fogarty, D.; Cooke, R.; Casadevall, C. D.; Salleo, A.; Parlak, O. Wearable Organic Electrochemical Transistor Patch for Multiplexed Sensing of Calcium and Ammonium Ions from Human Perspiration. *Adv. Healthc. Mater.* **2019**, *8* (24), 1−8.
(21) Fenoy, G. E.; Hasler, R.; Quartinello, F.; Marmisollé, W. A.; Lorenz, C.; Azzaroni, O.; Bäuerle, P.; Knoll, W. Clickable" Organic Electrochemical Transistors. *JACS Au* **2022**, *2* (12), 2778−2790.
(22) Huang, W.; Chen, J.; Yao, Y.; Zheng, D.; Ji, X.; Feng, L. W.; Moore, D.; Glavin, N. R.; Xie, M.; Chen, Y.; Pankow, R. M.; Surendran, A.; Wang, Z.; Xia, Y.; Bai, L.; Rivnay, J.; Ping, J.; Guo, X.; Cheng, Y.; Marks, T. J.; Facchetti, A. Vertical Organic Electrochemical Transistors for Complementary Circuits. *Nature* **2023**, *613* (7944), 496−502.
(23) Fenoy, G. E.; Hasler, R.; Lorenz, C.; Movilli, J.; Marmisollé, W. A.; Azzaroni, O.; Huskens, J.; Bäuerle, P.; Knoll, W. Interface Engineering of "Clickable" Organic Electrochemical Transistors toward Biosensing Devices. *ACS Appl. Mater. Interfaces* **2023**, *15* (8), 10885−10896.
(24) Zeglio, E.; Inganäs, O. Active Materials for Organic Electrochemical Transistors. *Adv. Mater.* **2018**, *30* (44), No. 1800941.
(25) Rivnay, J.; Leleux, P.; Ferro, M.; Sessolo, M.; Williamson, A.; Koutsouras, D. A.; Khodagholy, D.; Ramuz, M.; Strakosas, X.; Owens, R. M.; Benar, C.; Badier, J.-M.; Bernard, C.; Malliaras, G. G. High-Performance Transistors for Bioelectronics through Tuning of Channel Thickness. *Sci. Adv.* **2015**, *1* (4), No. e1400251.
(26) Inal, S.; Malliaras, G. G.; Rivnay, J. Benchmarking Organic Mixed Conductors for Transistors. *Nat. Commun.* **2017**, *8* (1), 1−6.
(27) Marks, A.; Griggs, S.; Gasparini, N.; Moser, M. Organic Electrochemical Transistors: An Emerging Technology for Biosensing. *Adv. Mater. Interfaces* **2022**, *9* (6), No. 2102039.
(28) Keene, S. T.; van der Pol, T. P. A.; Zakhidov, D.; Weijtens, C. H. L.; Janssen, R. A. J.; Salleo, A.; van de Burgt, Y. Enhancement-Mode PEDOT:PSS Organic Electrochemical Transistors Using Molecular De-Doping. *Adv. Mater.* **2020**, *32* (19), No. 2000270.
(29) Fenoy, G. E.; Azzaroni, O.; Knoll, W.; Marmisollé, W. A. Functionalization Strategies of PEDOT and PEDOT:PSS Films for Organic Bioelectronics Applications. *Chemosensors* **2021**, *9* (8), 212.
(30) Mantione, D.; del Agua, I.; Sanchez-Sanchez, A.; Mecerreyes, D. Poly(3,4-Ethylenedioxythiophene) (PEDOT) Derivatives: Innovative Conductive Polymers for Bioelectronics. *Polymers* **2017**, *9*, 354.
(31) Minudri, D.; Mantione, D.; Dominguez-Alfaro, A.; Moya, S.; Maza, E.; Bellacanzone, C.; Antognazza, M. R.; Mecerreyes, D. Water Soluble Cationic Poly(3,4-Ethylenedioxythiophene) PEDOT-N as a Versatile Conducting Polymer for Bioelectronics. *Adv. Electron. Mater.* **2020**, *6* (10), 1−10.

(32) Donahue, M. J.; Sanchez-Sanchez, A.; Inal, S.; Qu, J.; Owens, R. M.; Mecerreyes, D.; Malliaras, G. G.; Martin, D. C. Tailoring PEDOT Properties for Applications in Bioelectronics. *Mater. Sci. Eng. R Reports* **2020**, *140*, No. 100546.
(33) Buth, F.; Donner, A.; Sachsenhauser, M.; Stutzmann, M.; Garrido, J. A. Biofunctional Electrolyte-Gated Organic Field-Effect Transistors. *Adv. Mater.* **2012**, *24* (33), 4511−4517.
(34) Fenoy, G. E.; von Bilderling, C.; Knoll, W.; Azzaroni, O.; Marmisolle, W. A. PEDOT:Tosylate-Polyamine-Based Organic Electrochemical Transistors for High-Performance Bioelectronics. *Adv. Electron. Mater.* **2021**, *7* (6), No. 2100059.
(35) Montero-Jimenez, M.; Amante, F. L.; Fenoy, G. E.; Scotto, J.; Azzaroni, O.; Marmisolle, W. A. PEDOT-Polyamine-Based Organic Electrochemical Transistors for Monitoring Protein Binding. *Biosensors* **2023**, *13* (2), 288.
(36) Fenoy, G. E.; Scotto, J.; Allegretto, J. A.; Piccinini, E.; Cantillo, A. L.; Knoll, W.; Azzaroni, O.; Marmisollé, W. A. Layer-by-Layer Assembly Monitored by PEDOT-Polyamine-Based Organic Electrochemical Transistors. *ACS Appl. Electron. Mater.* **2022**, *4* (12), 5953−5962.
(37) Fenoy, G. E.; Piccinini, E.; Knoll, W.; Marmisollé, W. A.; Azzaroni, O. The Effect of Amino−Phosphate Interactions on the Biosensing Performance of Enzymatic Graphene Field-Effect Transistors. *Anal. Chem.* **2022**, *94* (40), 13820−13828.
(38) Mitobe, R.; Sasaki, Y.; Tang, W.; Zhou, Q.; Lyu, X.; Ohshiro, K.; Kamiko, M.; Minami, T. Multi-Oxyanion Detection by an Organic Field-Effect Transistor with Pattern Recognition Techniques and Its Application to Quantitative Phosphate Sensing in Human Blood Serum. *ACS Appl. Mater. Interfaces* **2022**, *14* (20), 22903−22911.
(39) Laucirica, G.; Pérez-Mitta, G.; Toimil-Molares, M. E.; Trautmann, C.; Marmisollé, W. A.; Azzaroni, O. Amine-Phosphate Specific Interactions within Nanochannels: Binding Behavior and Nanoconfinement Effects. *J. Phys. Chem. C* **2019**, *123* (47), 28997−29007.
(40) Sappia, L. D.; Piccinini, E.; von Binderling, C.; Knoll, W.; Marmisollé, W.; Azzaroni, O. PEDOT-Polyamine Composite Films for Bioelectrochemical Platforms - Flexible and Easy to Derivatize. *Mater. Sci. Eng., C* **2020**, *109*, No. 110575.
(41) Garreau, S.; Louarn, G.; Buisson, J. P.; Froyer, G.; Lefrant, S. In Situ Spectroelectrochemical Raman Studies of Poly (3, 4-Ethylenedioxythiophene)(PEDT). *Macromolecules* **1999**, *32* (20), 6807−6812.
(42) Sappia, L. D.; Piccinini, E.; Marmisollé, W.; Santilli, N.; Maza, E.; Moya, S.; Battaglini, F.; Madrid, R. E.; Azzaroni, O. Integration of Biorecognition Elements on PEDOT Platforms through Supramolecular Interactions. *Adv. Mater. Interfaces* **2017**, *4* (17), No. 1700502.
(43) Lee, S. H.; Park, H.; Kim, S.; Son, W.; Cheong, I. W.; Kim, J. H. Transparent and Flexible Organic Semiconductor Nanofilms with Enhanced Thermoelectric Efficiency. *J. Mater. Chem. A* **2014**, *2* (20), 7288−7294.
(44) Stavrinidou, E.; Winther-Jensen, O.; Shekibi, B. S.; Armel, V.; Rivnay, J.; Ismailova, E.; Sanaur, S.; Malliaras, G. G.; Winther-Jensen, B. Engineering Hydrophilic Conducting Composites with Enhanced Ion Mobility. *Phys. Chem. Chem. Phys.* **2014**, *16* (6), 2275−2279.
(45) Talukdar, H.; Bhowal, A. C.; Kundu, S. Percolation Dependent Conducting Behavior of Poly (3,4-Ethylenedioxythiophene): Poly (Styrenesulfonate) in the Presence of Cationic Polyelectrolyte. *Phys. E Low-dimensional Syst. Nanostructures* **2019**, *107*, 30−37.
(46) Keene, S. T.; van der Pol, T. P. A.; Zakhidov, D.; Weijtens, C. H. L.; Janssen, R. A. J.; Salleo, A.; van de Burgt, Y. Enhancement-Mode PEDOT:PSS Organic Electrochemical Transistors Using Molecular De-Doping. *Adv. Mater.* **2020**, *32* (19), No. 2000270.
(47) Van Der Pol, T. P. A.; Keene, S. T.; Saes, B. W. H.; Meskers, S. C. J.; Salleo, A.; Van De Burgt, Y.; Janssen, R. A. J. The Mechanism of Dedoping PEDOT:PSS by Aliphatic Polyamines. *J. Phys. Chem. C* **2019**, *123* (39), 24328−24337.
(48) Inal, S.; Rivnay, J.; Hofmann, A. I.; Uguz, I.; Mumtaz, M.; Katsigiannopoulos, D.; Brochon, C.; Cloutet, E.; Hadziioannou, G.; Malliaras, G. G. Organic Electrochemical Transistors Based on PEDOT with Different Anionic Polyelectrolyte Dopants. *J. Polym. Sci., Part B: Polym. Phys.* **2016**, *54* (2), 147−151.
(49) Giovannitti, A.; Nielsen, C. B.; Sbircea, D.-T.; Inal, S.; Donahue, M.; Niazi, M. R.; Hanifi, D. A.; Amassian, A.; Malliaras, G. G.; Rivnay, J.; McCulloch, I. N-Type Organic Electrochemical Transistors with Stability in Water. *Nat. Commun.* **2016**, *7* (1), 13066.
(50) Harman, D. G.; Gorkin, R.; Stevens, L.; Thompson, B.; Wagner, K.; Weng, B.; Chung, J. H. Y.; in het Panhuis, M.; Wallace, G. G. Poly(3,4-Ethylenedioxythiophene):Dextran Sulfate (PEDOT:DS) − A Highly Processable Conductive Organic Biopolymer. *Acta Biomater.* **2015**, *14*, 33−42.
(51) Cortez, M. L.; Lorenzo, A.; Marmisollé, W. A.; von Bilderling, C.; Maza, E.; Pietrasanta, L.; Battaglini, F.; Ceolín, M.; Azzaroni, O. Highly-Organized Stacked Multilayers via Layer-by-Layer Assembly of Lipid-like Surfactants and Polyelectrolytes. Stratified Supramolecular Structures for (Bio)Electrochemical Nanoarchitectonics. *Soft Matter* **2018**, *14* (10), 1939−1952.
(52) Marmisollé, W. A.; Irigoyen, J.; Gregurec, D.; Moya, S.; Azzaroni, O. Supramolecular Surface Chemistry: Substrate-independent, Phosphate-driven Growth of Polyamine-based Multifunctional Thin Films. *Adv. Funct. Mater.* **2015**, *25* (26), 4144−4152.
(53) Lorenzo, A.; Marmisollé, W. A.; Maza, E. M.; Ceolín, M.; Azzaroni, O. Electrochemical Nanoarchitectonics through Polyaminobenzylamine−Dodecyl Phosphate Complexes: Redox Activity and Mesoscopic Organization in Self-Assembled Nanofilms. *Phys. Chem. Chem. Phys.* **2018**, *20* (11), 7570−7578.
(54) Scotto, J.; Cantillo, A. L.; Piccinini, E.; Fenoy, G. E.; Allegretto, J. A.; Piccinini, J. M.; Marmisollé, W. A.; Azzaroni, O. Using Graphene Field-Effect Transistors for Real-Time Monitoring of Dynamic Processes at Sensing Interfaces. Benchmarking Performance against Surface Plasmon Resonance. *ACS Appl. Electron. Mater.* **2022**, *4* (8), 3988−3996.
(55) Piccinini, E.; Alberti, S.; Longo, G. S.; Berninger, T.; Breu, J.; Dostalek, J.; Azzaroni, O.; Knoll, W. Pushing the Boundaries of Interfacial Sensitivity in Graphene FET Sensors: Polyelectrolyte Multilayers Strongly Increase the Debye Screening Length. *J. Phys. Chem. C* **2018**, *122* (18), 10181−10188.
(56) Huang, Y.-C.; Liu, T.-J. Mobilization of Mesenchymal Stem Cells by Stromal Cell-Derived Factor-1 Released from Chitosan/Tripolyphosphate/Fucoidan Nanoparticles. *Acta Biomater.* **2012**, *8* (3), 1048−1056.
(57) Shu, X. Z.; Zhu, K. J. A Novel Approach to Prepare Tripolyphosphate/Chitosan Complex Beads for Controlled Release Drug Delivery. *Int. J. Pharm.* **2000**, *201* (1), 51−58.
(58) Sabirov, R. Z.; Okada, Y. ATP Release via Anion Channels. *Purinergic Signal.* **2005**, *1* (4), 311−328.
(59) Hong, S. U.; Malaisamy, R.; Bruening, M. L. Separation of Fluoride from Other Monovalent Anions Using Multilayer Polyelectrolyte Nanofiltration Membranes. *Langmuir* **2007**, *23* (4), 1716−1722.
(60) Capdevila, D. A.; Marmisollé, W. A.; Williams, F. J.; Murgida, D. H. Phosphate Mediated Adsorption and Electron Transfer of Cytochrome c. A Time-Resolved SERR Spectroelectrochemical Study. *Phys. Chem. Chem. Phys.* **2013**, *15* (15), 5386−5394.

https://doi.org/10.1021/acsami.3c09286
ACS Appl. Mater. Interfaces XXXX, XXX, XXX−XXX